Chemistry—Methods
Concept
doi.org/10.1002/cmtd.202400080
Chemistry Europe
European Chemical Societies Publishing
www.chemistrymethods.org

Wettability-Controlled Electrocatalytic Carbon Dioxide Reduction

Lanze Li, Jiexin Wen, Tsz Woon Benedict Lo,* Jun Yin,* and Qiong Lei*

The electrocatalytic CO_2 reduction reaction (eCO_2RR) offers a promising pathway for converting greenhouse gases into valuable fuels and chemicals using renewable energy. Beyond advancements in catalyst and electrolyzer design, significant opportunities lie in the strategic modulation of the gas–liquid–solid three-phase interface (TPI) on the catalyst surface. After revisiting the evolution from traditional liquid–solid double-phase interfaces to advanced gas–liquid–solid TPIs, this concept outlines major challenges in constructing stable TPIs on eCO_2RR gas diffusion electrodes and reviews recent progress in TPI modulation through hydrophobicity enhancement. Further, achieving a delicate balance between hydrophobicity and hydrophilicity—optimal wettability—is crucial for optimizing TPI construction, and enhancing overall electrocatalytic performance is emphasized. This work provides valuable insights for designing efficient TPIs in eCO_2RR and other gas-involved electrochemical processes, contributing to advancements in sustainable energy technologies.

1. Introduction

The rampant consumption of fossil fuels and the resulting CO_2 emissions have precipitated severe environmental challenges, such as climate change, sea-level rise, and ocean acidification, compelling extensive efforts to mitigate carbon emissions through strategies, like CO_2 capture, storage, and conversion.[1] Converting CO_2 into chemicals and fuels using low-carbon energy has become an appealing approach to leverage the extreme climate change as well as the growing energy needs.[2] Among different conversion techniques, the electrocatalytic CO_2 reduction reaction (eCO_2RR), especially when paired with renewable energy sources, such as solar and wind, emerge as a promising method due to its technical ease and minimal environmental impact, attracting considerable research interest from both academia and industry.[3]

The eCO_2RR is a complex process including multiple proton–electron transfer steps that yield a variety of products.[4] These products range from two-electron transferred products like formate/formic acid (HCOOH) and carbon monoxide (CO) to multi-electron transferred products, such as methane (CH_4), ethylene (C_2H_4), ethanol (C_2H_5OH), propanol (C_3H_7OH), etc.[5] Although current technologies can achieve high conversion for the former, it remains challenging for the latter products due to low selectivity and insufficient stability of the catalytic system, which hampers the economic viability of eCO_2RR.[6] To overcome these challenges, beyond advances in catalyst design and electrochemical cell configuration, significant opportunities remain relatively underexplored in the strategic modulation of the catalyst microenvironment.[7]

For highly efficient eCO_2RR, the microenvironment of catalytic sites is crucial as the reaction typically occurs at the three-phase interface (TPI), wherein gaseous CO_2 and liquid electrolytes come into intimate contact with the solid catalyst.[8] Such a TPI configuration allows direct delivery of gaseous CO_2 reactant to the catalytic sites and enables the usage of a range of electrolytes with different pH levels, significantly boosting the eCO_2RR electron transfer kinetics and paving the way for potential industrial-scale applications.[9] However, current configurations of TPI generally suffer from poor stability and imbalanced gas/liquid supply, which can diminish the eCO_2RR activity and hinder effective regulation of product selectivity.[10] The wettability of the catalyst surface—the ability of the liquid electrolyte to maintain consistent contact—is crucial for regulating the transport behavior of gas and liquid at the TPIs, directly impacting essential processes, such as gas diffusion and electron transfer. Therefore, wettability engineering has emerged as a powerful knob for regulating the catalytic rate and product selectivity in eCO_2RR.[11] Nonetheless, studying the TPI presents considerable challenges, with current knowledge on the interfacial structures and CO_2 transport behavior under nonequilibrium conditions remaining limited.[12] This scenario underscores the need for a critical overview of the reported engineering strategies and a deepened understanding of the wettability-controlled eCO_2RR.

L. Li, J. Wen, Q. Lei
Macao Institute of Materials Science and Engineering (MIMSE)
Macau University of Science and Technology
Taipa, Macao 999078, China
E-mail: qlei@must.edu.mo

T. W. B. Lo, J. Yin
Department of Applied Physics
The Hong Kong Polytechnic University
Kowloon, Hong Kong 999077, China
E-mail: benedict.tw.lo@polyu.edu.hk
jun.yin@polyu.edu.hk

T. W. B. Lo
Department of Applied Biology and Chemical Technology
The Hong Kong Polytechnic University
Kowloon, Hong Kong 999077, China

In this concept, we begin by tracing the evolution of catalytic interface configurations from traditional liquid–solid double-phase interface (DPI) to the contemporary gas–liquid–solid TPI in eCO_2RR. After listing the major challenges associated with constructing TPIs of eCO_2RR gas-diffusion electrodes (GDEs), we summarize recent advancements in managing TPI stability and enrichment to promote eCO_2RR performance, which include hydrophobic polymer/molecular modifications and the fabrication of hierarchical structures to enhance hydrophobicity. At the end, we discuss current trends and future opportunities in steering the eCO_2RR reaction rate, product selectivity, and system stability through wettability engineering. By exploring and optimizing the stable wettability of catalytic electrodes, we aim to unlock further possibilities for improving the performance of the eCO_2RR and other electrochemical processes involving gaseous reactants.

2. Evolution of Catalytic Interface Configurations in eCO_2RR

Traditionally, eCO_2RR was assessed using H-type cells, where solubilized CO_2 in aqueous electrolyte is employed as the reactant. During electrolysis, the working electrode is immersed in liquid electrolyte, while gaseous CO_2 molecules are dissolved and diffuse along a concentration gradient to reach the catalyst surface for reactions (**Scheme 1**a), forming liquid–solid DPI around the catalytic sites. Early studies with this cell configuration established the fundamental knowledge frame for this field, yet the reaction rate in such conditions is restrained due to the limited mass transport at higher current densities. This is caused by the low concentration of solubilized CO_2 ($0.033\ \mathrm{mol\,L^{-1}}$ at 25 °C) and sluggish diffusion of CO_2 in the aqueous electrolyte (diffusion coefficient $t_{CO_2} = 0.00176\ \mathrm{mm^2\,s^{-1}}$ at 20 °C).[2a] The limiting current density for eCO_2RR on a planar electrode can be calculated using the formula $j_{\mathrm{lim}} = \frac{nFD_0C_0}{\delta}$, where n represents the number of electrons transferred during the reaction, F represents the Faraday constant, D_0 and C_0 represent the diffusion coefficient and solubility of CO_2 in the electrolyte, respectively, and δ represents the diffusion layer thickness.[13] This diffusion layer represents the interval over in which the CO_2 concentration gradient decreases from the electrode surface to the bulk concentration. For eCO_2RR in an H-cell, the diffusion layer thickness is on the order of 100 μm, leading to a typical limiting current density around 30–35 $\mathrm{mA\,cm^{-2}}$.

To alleviate these mass transport limitations, GDEs-based flow cells and membrane electrode assemblies (MEAs) have been developed and are now widely used to study eCO_2RR. A standard GDE comprises two key parts: a gas diffusion layer (GDL, typically a dense network of carbon fibers in form of carbon paper/cloth or a polytetrafluoroethylene (PTFE) membrane), and the catalyst layer. For carbon-based GDL, an additional microporous layer (MPL) is commonly sandwiched between the other two layers to prevent the catalyst from excess water. The catalyst-laden side of the GDE interfaces with the electrolyte, while the other side is exposed to CO_2 gas stream. The gaseous CO_2 diffuses through the pores of the GDL and can directly reach the catalyst, forming a gas–liquid–solid TPI, where gaseous CO_2 and liquid electrolytes come into close contact and react on the surface of the solid catalyst (Scheme 1b). This configuration significantly enhances CO_2

Lanze Li obtained his Master's degree in Mechanical Engineering from Zhejiang A&F University in 2023. He is currently a first-year Ph.D. student at the Macau University of Science and Technology under the supervision of Prof. Qiong Lei. His research mainly focuses on the electrocatalytic reduction of carbon dioxide and zinc-based energy storage devices.

Jiexin Wen graduated from Hubei University of Technology with a Master's degree in Materials Science in 2024. She is currently a first-year Ph.D. student at Macau University of Science and Technology under the supervision of Prof. Qiong Lei. Her research mainly focuses on electrocatalytic reduction of carbon dioxide and aqueous zinc-ion batteries.

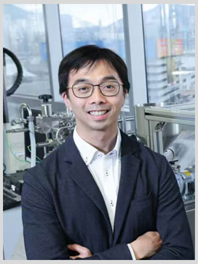

Tsz Woon Benedict Lo's research has significantly advanced the understanding of zeolite catalysts, providing a foundation for developing more efficient and sustainable catalytic processes. By addressing the fundamental challenges in characterizing active site distributions, his research has opened new avenues for designing catalysts with enhanced performance and reduced environmental impact.

Jun Yin is an Assistant Professor in the Department of Applied Physics at The Hong Kong Polytechnic University with a conferred title of Presidential Young Scholar. His research group specializes in the development of theoretical models and multi-scale simulation methodologies to understand catalytic reaction mechanisms in nanomaterial systems. He has published over 230 SCI-indexed papers with an h-index of 73. He was recognized as one of the top 2% most-cited scientists worldwide (2022-2024) by Stanford University.

Qiong Lei is an Assistant Professor in the Macao Institute of Materials Science and Engineering (MIMSE) at Macau University of Science and Technology. Her research group specializes in the reactor and material engineering for electrocatalytic storage and conversion (e.g., CO_2 reduction and ammonia synthesis), with a strong emphasis on integrating advanced operando characterization techniques with computational modeling to investigate reaction mechanisms.

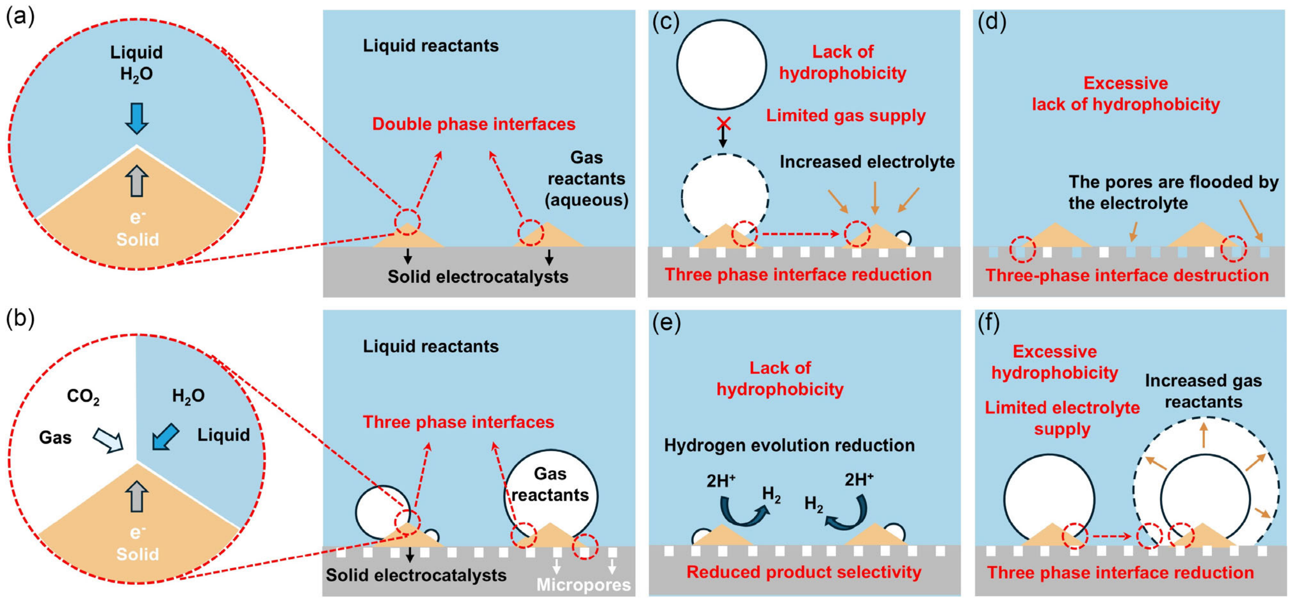

Scheme 1. Schematic diagram of a) the liquid–solid DPI and b) the gas–liquid–solid TPI. Schematic illustration of challenges confronted by TPIs due to lack of hydrophobicity: c) reduction of TPI caused by limited gas supply and increased electrolyte, d) flooding and destruction of the TPI due to MPL blockage by excessive electrolyte, and e) decreased eCO_2RR product selectivity resulting from competitive hydrogen evolution reactions (HER). Illustration of issues arising from excessive hydrophobicity of TPI: f) Transformation of TPI into gas–liquid and gas–solid interfaces due to gas enrichment and limited electrolyte transport, leading to a reduction in TPI. Reproduced with permission.[11] Copyright 2024, The Royal Society of Chemistry.

transport to the catalytic sites for efficient proton–electron transfer, allowing for industrial relevant current densities well above 100 mA cm^{-2} and the potential stacking of electrolyzers in large scale applications. Adoption of TPI in eCO_2RR has initiated a new era with new design guidelines and operating principles, achieving performance levels that align with commercial expectations.[13] To date, the partial current densities for ethylene and carbon monoxide production hit ampere level,[14] similar to those of commercial water electrolysis reactors.

Apart from increasing reaction current density, TPI also provides a platform to regulate catalytic activity,[15,16] product selectivity,[17] and stability[6,18] through varying the supply of CO_2 and protons. For example, Han et al. demonstrated that the CO_2/proton ratio can be modulated by controlling the accessibility of water to the TPI on the copper-based catalyst surface, and that a change in the CO_2/H_2O ratio can enable a reaction path switch from ethylene to ethanol (**Figure 1**a).[19] This occurs primarily because the modulation of TPI alters the coverage of *CO and *H, subsequently influencing the kinetics of proton transfer and ultimately affecting the catalytic activity and product selectivity. Li et al. optimized the gas–catalyst–electrolyte TPI to enhance active site exposure and improve mass/charge transport, while preventing electrolyte flooding during eCO_2RR on an indium nanosheets electrode.[20] By enabling control over the local concentrations of CO_2 and protons and facilitating the formation and stabilization of $CO_2{}^{*-}$ intermediates, this approach achieved a remarkable Faradaic efficiency (FE) of 96.3% toward formate with a maximum partial current density over 360 mA cm^{-2} and negligible selectivity degradation after 140 h of operation in 10020M KOH solution, surpassing the state-of-the-art indium-based electrocatalysts (Figure 1b,c). Both examples illustrate the pivotal role of TPI in eCO_2RR catalytic performance.

3. Current Challenges of TPIs in eCO_2RR

Although the implementation of TPI in GDE-based flow cells and MEA has greatly enhanced the eCO_2RR performance, there are still challenges remaining. 1) In GDEs, the catalyst particles are easily wetted by the electrolyte during electrochemical reaction due to the lack of hydrophobicity, which damages the TPI and decreases the catalytic efficiency (Scheme 1c).[21] For example, Cross et al. examined reactions involving gas–liquid phases on the surface of several solid catalysts, emphasizing that the wettability of nanostructured materials plays a crucial role in their effectiveness as catalysts.[22] Excessive wetting of the catalyst surface by liquid reactants can diminish the number of active sites, subsequently compromising the catalytic activity; 2) In more severe cases, the electrolyte may flood the pores of the GDE, which can cause destruction of the TPI, serving as the major degradation factor for eCO_2RR electrolyzer in high current density operation (Scheme 1d).[23] Through systematic investigation on the flooding behavior during the eCO_2RR, Vermaas et al. found that when the hydrophobicity of TPI is insufficient, the liquid pressure gradually increases until it surpasses the capillary force, leading to the infiltration of electrolyte into the pore network, and thereby flooding.[10] This work highlights that enhancing hydrophobicity is critical for improving the TPI stability; 3) When the TPI structure is compromised due to hydrophobicity deficiencies, the catalytic sites experience CO_2 shortage caused by gas mass transfer limitations, similar to the DPI situation. Under such conditions, the kinetically favored HER rapidly dominates over eCO_2RR by severely impairing both the activity and selectivity, especially at elevated current densities (Scheme 1e).[24] Mougel's study revealed that using a nonhydrophobic GDE for eCO_2RR resulted

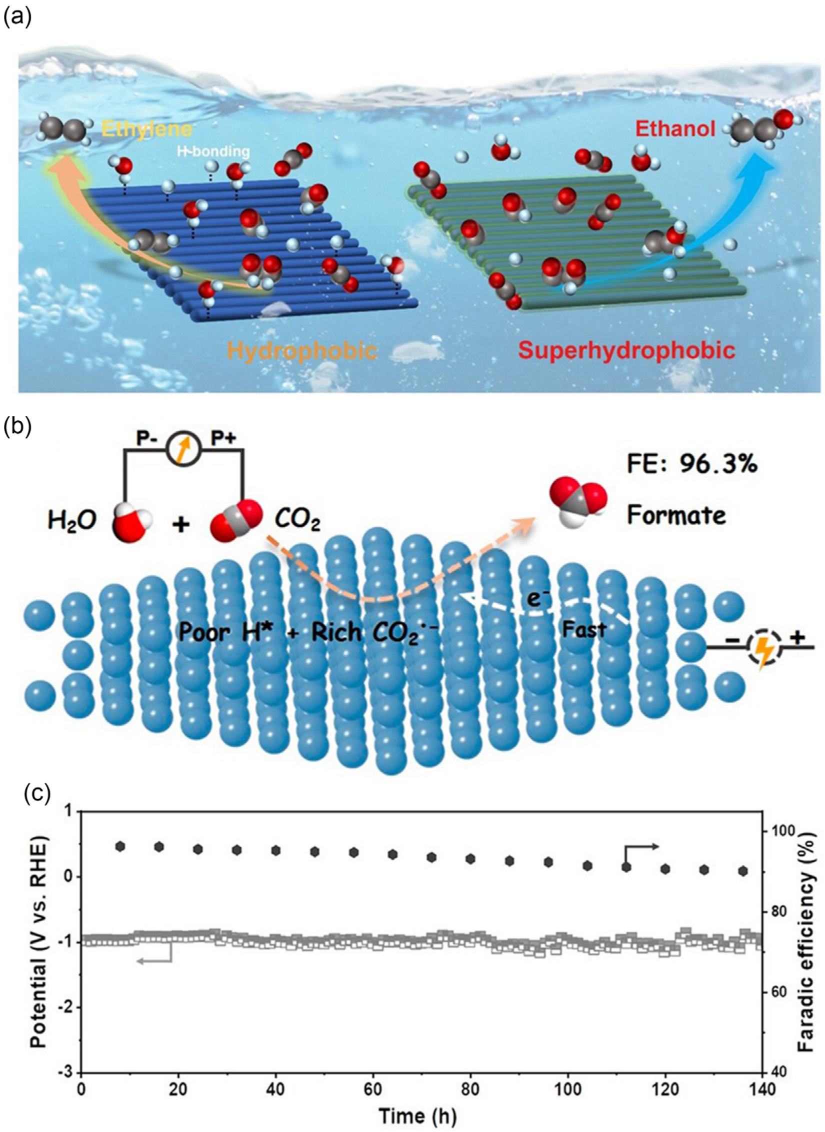

Figure 1. a) Schematic diagram of the transition of the reaction pathway from ethylene to ethanol achieved through polypyrrole coating on the surface of a copper (Cu)-based catalyst. The polypyrrole coating on the TPI increases the CO_2/proton ratio, thereby enabling the regulation of catalytic activity and product selectivity. Reproduced with permission.[19] Copyright 2024, Wiley-VCH. b) Schematic diagram of regulating the CO_2/proton ratio at the TPI by adjusting the gas–liquid pressure difference on the surface of the indium nanosheets electrode. c) Stability test of the indium nanosheets electrode at -100 mA cm^{-2}. Reproduced with permission.[20] Copyright 2023, American Chemical Society.

in FE of 24% for eCO_2RR products and 71% for H_2; whilst its hydrophobically modified counterpart effectively enhanced the FE for eCO_2RR to 71%, suppressing that of HER within 10%.[19b] These findings underscore the significant role of TPI structure in regulating eCO_2RR competence over the HER; 4) In certain cases, although the hydrophobicity around the catalyst surface is reinforced prior to the reaction, it may gradually diminish along the eCO_2RR process as the applied electric field promotes liquid diffusion, ultimately disrupting the TPI.[25] For example, Sargent et al. assessed the surface wettability of bare carbon GDEs and observed a decrease in the contact angle from 145° to 117° after 1 h of operation at -0.8 V_{RHE} (**Table 1**), suggesting the degradation of the electrode hydrophobicity under the influence of the electric field.[26] Electrowetting management remains a significant hurdle for building stable TPI configurations.

These analyses highlight that, in addition to electrocatalyst engineering, the construction of a stable TPI is crucial for achieving high activity, selectivity, and stability in eCO_2RR.[11] Moreover, the current challenges with TPI deficiency primarily stem from insufficient hydrophobicity on the catalyst surface, underscoring the need for strategic control over the gas–liquid–solid TPI, particularly through tailoring the hydrophobicity of the electrodes.

4. Hydrophobicity Engineering in eCO_2RR

To address the challenges associated with TPI deficiency, it is essential to develop effective strategies for enhancing the hydrophobicity of the catalytic interface. Significant progress has been made in regulating hydrophobicity within the TPI, leading to

Table 1. GDEs and their water contact angle after hydrophobic modification via different methods.

Sample name	Modification method	Water contact angle (after performance testing)	Ref
Cu/CuO/Polypyrrole@CP	Polypyrrole coating	154°	[19]
Ag/PTFE-QAPPT@CP	PTFE-QAPPT	129.6°	[34]
CuO/PVDF@CP	PVDF coating	126.4°	[29]
Cu/SiO_2@GDL	SiO_2 coating	140° (140°)	[31]
Cu/1-octadecanethiol@GDL	1-octadecanethiol coating	150.4° (134.5°)	[35]
Cu/1-octadecanethiol@CP	1-octadecanethiol coating	153° (143°)	[19b]
CuO/Nafion@Cu	Nafion coating	127.11°	[32]
Cu/PTFE@CP	PTFE doping	150.8° (144.7°)	[15]
BiOOH/PTFE@CP	PTFE doping	161°	[16]
Cu/PTFE@ Cu foil	PTFE doping	152° ± 7°	[47]
Ni-N_4/CF_2@GDL	—CF_2— group doping	156.3	[34]
Ag/Lipid ligands@GDL	Lipid ligand doping	/	[39]
CoPc-NH_2/octadecylamine (ODA)@CNT	ODA doping	151.4° (140.7°)	[48]
$Cu(OH)_2$/Nafion@CP	Nafion doping	108.3	[49]
Au/PDMS@CP	PDMS doping	123°	[30]
Cu dendrite@CP	Needle-shaped microstructure	154°	[50]
Cu dendrite@Ti mesh	Sharp layered structure	/	[42]
Cu dendrite@CP	Sharp layered structure	167.9° (166.6°)	[51]

substantial improvements in the mass transfer processes and reactant affinity.[27] Consequently, the catalytic performance, including activity, selectivity, and stability, toward eCO_2RR can be effectively modulated via well-designed surface hydrophobic modifications.[27] In this section, we categorize the methodologies for constructing hydrophobic interfaces into two main approaches: hydrophobic polymer/molecule modification and hierarchical structure fabrication.

4.1. Hydrophobic Polymer/Molecular Modification

Recently, utilizing interactions between hydrophobic polymeric or molecular species and catalyst surfaces have been demonstrated as an effective strategy for introducing hydrophobicity into GDEs. Specifically, it involves decorating the catalyst surface with hydrophobic organic molecules through methods, such as electrochemical deposition, chemical grafting, or ligand attachment. Commonly utilized hydrophobic materials, include polypyrrole,[1a] PTFE,[15,28] polyvinylidene fluoride (PVDF),[29] polydimethylsiloxane (PDMS),[30] SiO_2,[31] 1-octadecanethiol,[19b] and ionomers, such as Nafion,[32] Fumion,[6] Imidazolium.[33] These materials possess low surface free energy, imparting them with hydrophobic properties, and are frequently used to regulate the hydrophobicity of catalyst surfaces.

4.1.1. Coating

Coating the catalyst surface with hydrophobic polymers has proven to be an effective strategy for suppressing HER and enhancing product selectivity. For instance, coating Cu nanofibers with a conductive polypyrrole creates a superhydrophobic Cu/$Cu_{2+1}O$/SHNC electrode, effectively weakening the hydrogen bonding interactions between interfacial water molecules (**Figure 2**a).[19] By facilitating the transfer of CO_2 and enhancing the local CO_2/H_2O ratio, this innovative electrode design exhibited exceptional selectivity for ethanol with a FE of 66.5% at $-1.1\ V_{RHE}$ in the flow cell (Figure 2b).[28] Zhao et al. investigated the impact of the electrode–electrolyte interface on eCO_2RR in acidic electrolyte by coating Ag electrodes with a hydrophobic cation-ionomer modification layer composed of quaternary ammonia poly (N-methyl-piperidine-co-p-terphenyl) (QAPPT) and PTFE (PTFE-Q electrode), and found that PTFE significantly enhanced the hydrophobicity of the GDE by restricting water diffusion and maintaining a higher local pH near the electrode surface.[34] This PTFE-Q electrode achieved a maximum FE of 95.6% toward CO at $100\ mA\ cm^{-2}$ in an acidic anolyte ($0.1\ mmol\ L^{-1}\ H_2SO_4$) with a low concentration of alkali–metal ions ($0.1\ mol\ L^{-1}\ K_2SO_4$).

In addition to polymers, hydrophobic molecules are also employed for this purpose. Wang et al. introduced an "armor protection" strategy by depositing an ultrathin hydrophobic SiO_2 layer onto the Cu surface (Cu/SiO_2), effectively imparting hydrophobicity, while preventing structural reconstruction of Cu and preserving the oxidation state of $Cu^{\delta+}$ active sites during eCO_2RR (Figure 2c).[31] The ultrathin SiO_2 layer also inhibited the accumulation of K^+ ions on the catalyst surface and restricted the diffusion of in situ generated OH^- ions away from the electrode, thereby promoting the generation of C_{2+} products. This approach achieved an impressive C_{2+} FE of 76.9% at $900\ mA\ cm^{-2}$ under strongly acidic conditions ($pH = 1$). Sun et al. imparted water-barrier properties on the porous Cu surface by coating with 1-octadecanethiol, resulting in a superhydrophobic Cu-GDL, which provided an FE of 87% toward C_{2+} products at a partial current density of $-1.6\ A\ cm^{-2}$ during acidic eCO_2RR (Figure 2d,e).[35]

This method involves covering the catalyst surface with hydrophobic polymers (e.g., PTFE, PVDF, PDMS) to form a

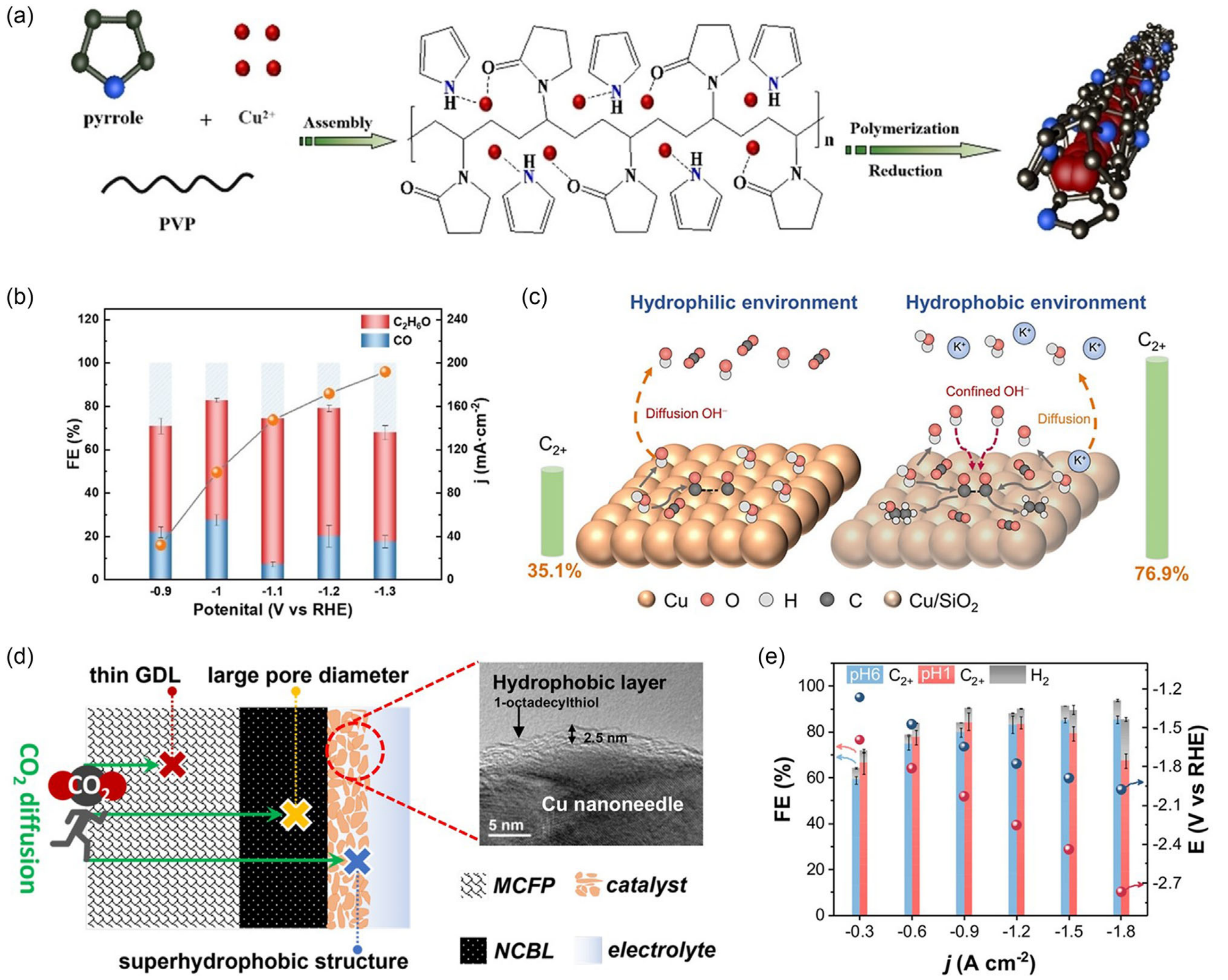

Figure 2. a) Illustration of the preparation process of Cu/$Cu_{2+1}O$/SHNC electrode. b) FE of different products and current density at different potentials during eCO_2RR with Cu/$Cu_{2+1}O$/SHNC electrode in a flow cell. Reproduced with permission.[19] Copyright 2024, Wiley-VCH. c) Illustration of the Cu catalyst surface with and without the ultrathin SiO_2 layer, forming a hydrophobic and hydrophilic environment, respectively, and the corresponding FE for C_{2+} products. Reproduced with permission.[31] Copyright 2023, American Chemical Society. d) Illustration of the superhydrophobic Cu-GDL and the corresponding transmission electron microscope image for the Cu nanoneedle catalyst covered with a 1-octadecylthiol single layer. e) The FE of C_{2+} products and H_2 and potential at different current densities. Reproduced with permission.[35] Copyright 2024, Springer Nature.

protective hydrophobic layer. Typically, it is achieved via spray coating, dip coating, or spin coating, standing out as a simple and scalable fabrication process. The use of chemically inert polymers, such as PTFE, which exhibit strong resistance to degradation in highly acidic or alkaline environments, also ensures excellent chemical stability. However, several limitations should be considered. Excessive coating may block catalytic active sites, and thereby reducing the electrochemically active surface area, and the added layer can increase interfacial resistance, potentially hindering electron transfer and lowering catalytic efficiency. Moreover, long-term operation may lead to adhesion issues, including delamination of the coating due to mechanical or electrochemical stress. Another challenge lies in the limited tunability of wettability, as most studies rely on a single polymer and modulate wettability primarily through thickness control, often resulting in very high or even superhydrophobic contact angles. Incorporating a mixture of polymers with varying intrinsic wettability may offer a more flexible and effective tuning strategy. This method is particularly well-suited for high gas flux conditions, such as high current density eCO_2RR ($>100\,mA\,cm^{-2}$), where robust hydrophobicity facilitates stable gas transport. It is also beneficial for hydrophilic catalyst systems, such as metal oxides and carbon-based materials, whose interfacial properties can be significantly enhanced through additional hydrophobic or superwetting[36] surface modifications to ensure an adequate supply of reactants.

4.1.2. Doping

To expand the TPI area for higher catalytic activity, while inhibiting HER, interdoping of polymer/molecule, and catalysts emerges as a promising method. Xing et al. developed a Cu/C/PTFE GDE with a hydrophobic microenvironment for eCO_2RR by dispersing PTFE nanoparticles inside the Cu nanocatalyst layer (**Figure 3**a).[15] By repelling the liquid electrolyte and maintaining gaseous CO_2

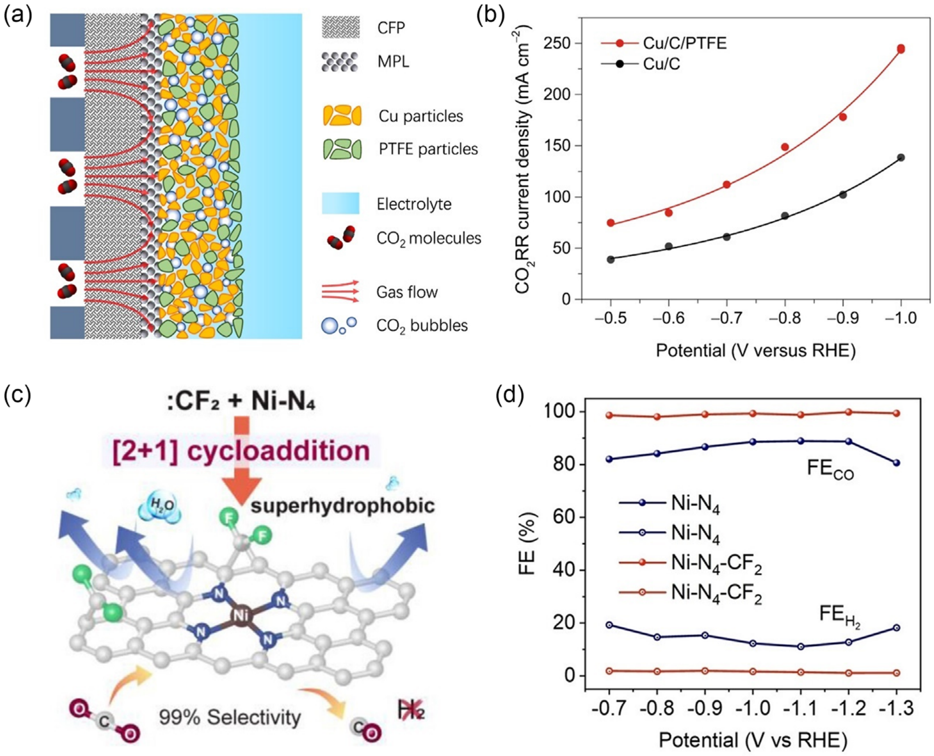

Figure 3. a) Illustration of the Cu/C/PTFE GDE configuration. b) eCO_2RR partial current density of the Cu/C/PTFE and Cu/C GDE electrodes at different potentials. Reproduced with permission.[15] Copyright 2021, Springer Nature. c) Illustration of the superhydrophobic Ni–N_4–CF_2 catalyst. d) FE of CO and H_2 at different potentials during eCO_2RR with the Ni–N_4–CF_2 and Ni–N_4 electrodes. Reproduced with permission.[38] Copyright 2024, Wiley-VCH.

near the catalyst particles, the PTFE-modified electrode creates a microenvironment with balanced CO_2 and electrolyte supply, effectively stabilizing and maximizing the TPI active sites within the catalyst layer. This significantly improves the mass transport and kinetics of CO_2 electrolysis, resulting in enhanced activity and selectivity for multicarbon (C_{2+}) products with a partial current density exceeding 250 mA cm^{-2} at moderate potentials, which approximately double that of the PTFE-free counterpart (Figure 3b). Building on this concept, Sheng et al. also engineered the TPI of a Ni–N–C catalyst for acidic eCO_2RR and achieved unit conversion to CO and a high single-pass CO_2 utilization of 75.7% at 200 mA cm^{-2},[37] demonstrating the broad applicability of this approach in enriching TPI active sites and boosting eCO_2RR activity.

Interdoping of polymer/molecule can also be realized by incorporating hydrophobic materials onto the catalysts as functional ligands. Shu et al. introduced difluorocarbene (F_2C:) into the hydrophilic Ni–N_4 single-atom catalyst, enabling surface fluorocarbonation and forming a superhydrophobic Ni–N_4–CF_2 electrode (Figure 3c).[38] Owing to the highly hydrophobic microenvironment created by the $-CF_2-$ group, the HER was significantly inhibited and an enhanced FE of over 98% for CO production across a wide operating potential range from -0.7 to -1.3 V_{RHE} (Figure 3d). Ko et al. reported that partially ligand-derived Ag nanoparticles (Ag-NPs) facilitate the smooth formation of TPI, preventing electrolyte flooding and ensuring efficient mass transfer of gaseous CO_2 for eCO_2RR (**Figure 4**b).[39] The lipid ligands prevent the splitting and detachment of Ag particles, ensuring consistent hydrophobicity retention in the Ag-NP electrode, even at high cathodic overpotentials. This results in $>$90% FE for CO at a partial current density of 298.39 mA cm^{-2} under a harsh applied potential of 3.4 V (Figure 4a).

Besides the aforementioned modification strategy of intermixing hydrophobic polymers/molecules/functional groups with catalysts, premodifying the GDE substrate with hydrophobic properties is also a viable approach. For instance, Park et al. prepared carbon GDEs with varying hydrophobicity by treating the carbon substrate with PDMS and doping the catalyst onto the substrate through sputtering (Figure 4c).[30] Compared with the hydrophobic and hydrophilic counterparts, the superhydrophobic Au electrode yielded better formation of TPI and exhibited a high FE of 94% toward CO production and a CO/H_2 ratio of 31:3 at a cathode potential of -0.7 V_{RHE} (Figure 4d).

This strategy involves physically or chemically incorporating hydrophobic agents (e.g., carbon black, PTFE particles) into the catalyst matrix to form a composite electrode. Compared to surface coatings, this approach offers a more uniform distribution of hydrophobicity, minimizing local wettability inhomogeneities, and better preserving access to catalytic active sites. Additionally, the inclusion of conductive materials like carbon black can enhance electron transport pathways, improving overall conductivity. However, this method also presents several challenges. Optimizing the doping ratio and mixing technique requires careful control to avoid structural inconsistency, and excessive incorporation of hydrophobic agents may compromise the mechanical integrity of the electrode. Furthermore, long-term operation can

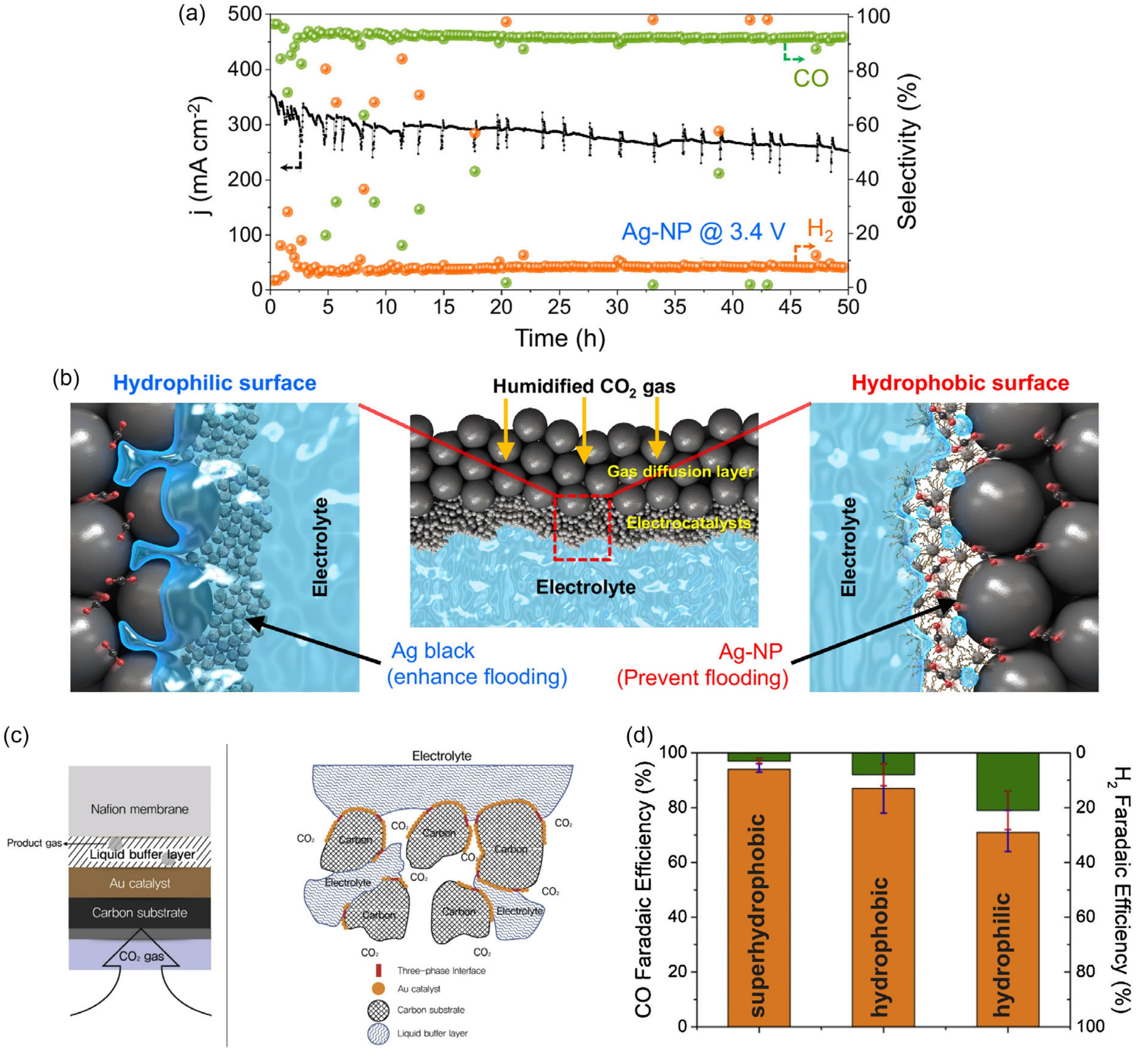

Figure 4. a) Stability test of the Ag-NP catalyst in a zero-gap CO_2 electrolyzer at 3.4 V for 50 h. b) Schematics of the TPI for the designed hydrophobic Ag-NP catalyst and the hydrophilic Ag black counterpart. Reproduced with permission.[39] Copyright 2024, Springer Nature. c) Illustration of gaseous CO_2 supply to the Au catalyst (left) and the TPI at the superhydrophobic Au electrode surface (right). d) FE of CO and H_2 during eCO_2RR with electrodes of different hydrophobicity. Reproduced with permission.[30] Copyright 2019, Elsevier B.V.

result in gradual electrolyte infiltration, leading to a decline in hydrophobic performance overtime. This strategy is particularly suitable for medium current density eCO_2RR, where a balance between gas and electrolyte transport is critical, and for catalyst systems with inherently low conductivity that benefit from the introduction of conductive additives.

4.2. Hierarchical Structure Fabrication for Hydrophobicity Building

Chemical modifications, such as attaching hydrophobic polymers or molecules, face notable limitations, including the potential to compromise the catalyst's inherent advantages by shielding active sites, reducing electrical conductivity, and being prone to washout during the reaction process.[40] In contrast, nature offers ingenious strategies for achieving hydrophobicity to trap gases while repelling water, forming proper gas–liquid–solid TPI for organisms survival. Ranging from lotus leaves to water spiders, these natural hydrophobic surfaces rely on hierarchical micro- and nanoscale structures that create sufficient roughness.[41] Inspired by these natural phenomena, researchers have developed novel hierarchical structures to engineer the TPI in GDEs, significantly enhancing eCO_2RR performance.

For instance, Niu et al. reported a hydrophobic Cu catalyst (Cu dendrites (Cu-D)) with a similar hierarchical structure of *Setaria* leaves, providing a sufficient hydrophobicity to establish a robust TPI that ensures efficient CO_2 mass transport and resists flooding (**Figure 5**a).[24] This design achieved an impressive FE of 64% toward C_{2+} production at 255 mA cm^{-2}, along with exceptional operational stability at 300 mA cm^{-2} for over 45 h in a flow cell, significantly outperforming the wettable

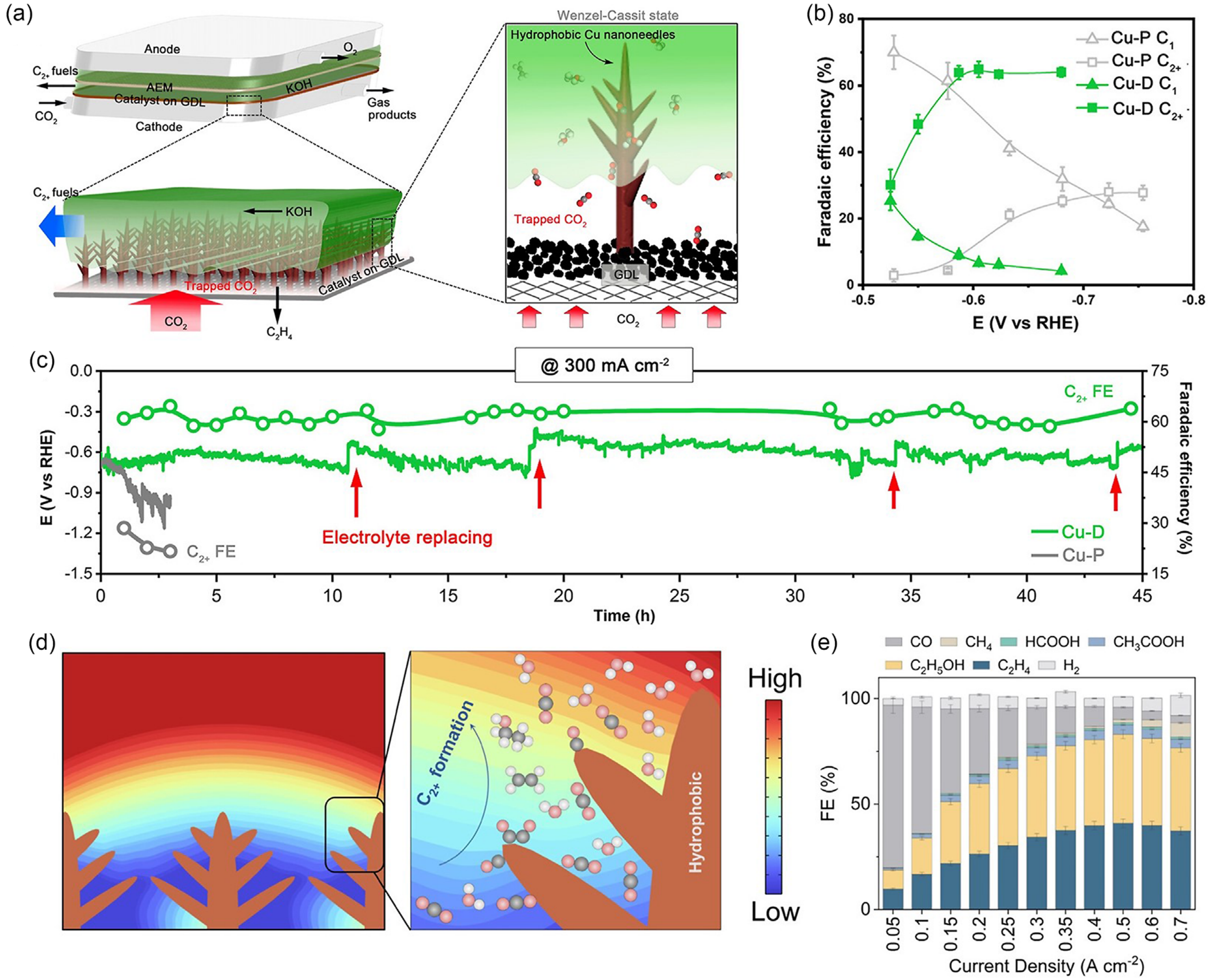

Figure 5. a) Illustration of the microfluidic CO_2 flow cell (left) and the stable gas–liquid–solid TPI enabled by the *Setaria*-inspired hierarchical Cu-D electrode design (right). b) FEs for C_{2+} and C_1 products on the Cu-D and wettable Cu-P electrodes during eCO_2RR at different potentials in a flow cell. c) Stability test of the Cu-D and Cu-P electrodes at a total current density of 300 mA cm^{-2}. Reproduced with permission.[24] Copyright 2021, American Chemical Society. d) Illustration of the stable gas–liquid–solid TPI enabled by the hierarchical Cu CF electrode design. e) FEs for various products on the Cu CF electrode during eCO_2RR at different current densities. Reproduced with permission.[42] Copyright 2023, American Chemical Society.

counterparts (Cu particles (Cu-P), Figure 5b,c). Similarly, Fang et al. developed a Cu dendrite electrode (Cu dendrites with an ultrastable $Cu^{\delta+}$ state and hydrophobicity (Cu CF)), where Cu(II) carboxylate coordination species were formed to induce an ultrastable $Cu^{\delta+}$ state and enhanced hydrophobicity, and observed a remarkable C_2 FE of 90.6% at a partial current density of 453.3 mA cm^{-2} in a flow cell (Figure 5d,e).[42] When tested in MEA, the electrode demonstrated stable electrolysis for 400 h at 800 mA and even achieved groundbreaking stability during operation at a large industrial current of 10 A. In short, hierarchical structure fabrication has proven to be particularly effective for generating abundant active sites while imparting exceptional hydrophobicity to stabilize the TPI for substantial eCO_2RR performance improvement.

This method modulates wettability by engineering micro- or nanoscale structural features (e.g., porous carbon fibers, hierarchical channels, bioinspired surface roughness) rather than introducing additional hydrophobic agents. Wettability is governed by intrinsic structural parameters like surface roughness and porosity, which not only eliminate the risk of chemical degradation or detachment but also offers strong structural stability over extended operational periods. Further, the increased surface area of micro/nanostructured materials provides more active sites, thereby enhancing catalytic efficiency. However, the fabrication of such structures often relies on sophisticated techniques, including templating, 3D printing, or vapor deposition, which can increase both process complexity and production cost. In addition, tuning wettability through structure alone requires precise control to avoid uneven electrolyte infiltration and maintains consistent interface performance. This approach is particularly advantageous in scenarios that demand long-term structural robustness, such as extended electrochemical operations, and is also well-suited for flexible or wearable devices, where both mechanical flexibility and tailored surface wettability are critical.

5. Outlook for Wettability-Controlled eCO_2RR.

For eCO_2RR, maintaining a balanced supply of gaseous CO_2 and liquid electrolyte onto the solid catalyst surface is crucial for optimizing the performance. It is widely recognized that excessively hydrophilic surfaces can lead to undesirable wetting, gas delivery blockages, and electrode flooding. However, it is less noticed that overly hydrophobic surfaces can repel the electrolyte excessively, limiting proton supply and adversely affecting reaction performance.[43] Both extremes impede the formation of a stable TPI, preventing the catalyst from achieving its optimal performance (Scheme 1f). Therefore, maintaining a delicate balance between hydrophobicity and hydrophilicity, namely an optimal wettability, plays a pivotal role in determining the catalytic performance of eCO_2RR.

Some researchers have practiced the above guideline and pioneered wettability engineering to modulate the TPI in eCO_2RR. For instance, Rabiee et al. developed a novel wettability modulation strategy by coating a Bi catalyst onto one layer of a double-layer flow-through hollow fiber GDE, creating distinct hydrophilic–hydrophobic regions (**Figure 6**a).[43] This design surpasses fully hydrophobic surfaces by facilitating mass transport, promoting TPI formation, and maximizing active sites. The strategy demonstrates stable wettability under eCO_2RR cathode

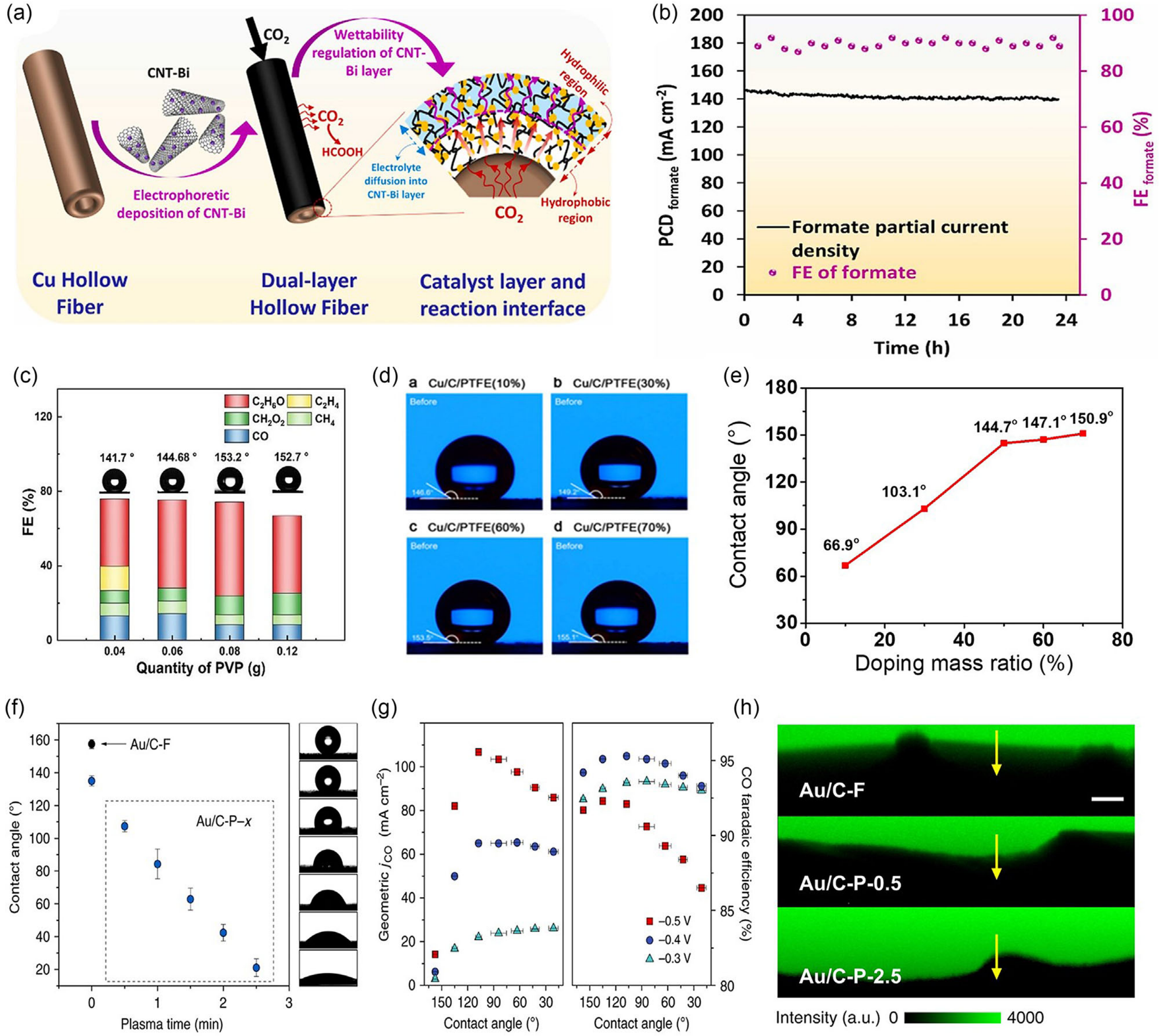

Figure 6. a) Schematic of dual-layer hollow fiber (HF) GDE fabrication with distinctive hydrophilic–hydrophobic regions and triple-phase-rich interfaces. b) Stability test of HFGDE at $-1.0\,V_{RHE}$ in a flow reactor. Reproduced with permission.[46] Copyright 2022, Elsevier B.V. c) FE for different products on the Cu CF electrode during eCO_2RR. Reproduced with permission.[19] Copyright 2024, Wiley-VCH. d) Contact angle measurements on the Cu/C/PTFE electrodes with various PTFE loadings before eCO_2RR at $-1.0\,V_{RHE}$ in the GDE cell, and e) the corresponding relationship between contact angles with PTFE doping mass ratio. Reproduced with permission.[15] Copyright 2021, Springer Nature. f) Plot of average water droplet contact angles on different Au/C electrodes and photographs of water droplets on each electrode. g) Geometric partial current density (j_{CO}) and FE for CO of Au/C electrodes with different water contact angles at various potentials. h) Cross-sectional fluorescence images of chosen regions on different Au/C electrodes. Reproduced with permission.[43] Copyright 2020, Springer Nature.

conditions, as evidenced by direct penetration depth measurements. Compared to untreated electrodes, the wettability-modulated electrodes obtained a catalyst utilization rate exceeding 80% and a fourfold increase in formate partial current density ($\approx$150 mA cm^{-2}, FE $>$90%), outperforming other GDEs used for formate production in CO_2RR under the same bicarbonate concentration (Figure 6b).

Through a statistical analysis summarized in Table 1, we find most of the contact angles in above mentioned studies exceed 150°, which correlate to superhydrophobicity. Although these strategies have proven to be effective in enhancing the activity, selectivity, and stability of eCO_2RR, excessively high hydrophobicity can introduce new challenges. Here, we examine the factors contributing to excessively high hydrophobicity in some of the aforementioned modification strategies and propose improvement approaches to address the associated limitations and challenges. 1) In research aimed at reducing HER, increasing hydrophobicity consistently leads to stronger HER suppression. While this may cause some disruption to the initial TPI (Scheme 1f), the overall impact can still improve product selectivity if the suppression of HER outweighs any adverse effects on eCO_2RR.[9] This approach effectively inhibits HER and enhances the stability of GDEs, and it could achieve even better catalytic performance when combined with strategies for optimizing TPI construction; 2) In studies regulating the TPI of eCO_2RR through hydrophobicity, the independent variable was always the doping amount of polymers or molecules rather than hydrophobicity or wettability of the interface itself (Figure 6c–e). As a result, even when polymer doping is scaled (Figure 6c, PVP doping from 40% to 120%;[24] Figure 6d,e PTFE doping from 10% to 70%[15]), the corresponding modulation of wettability is either limited (e.g., the contact angles concentrated in a narrow range of 141.7°–152.7° in Figure 6c) or unpredictable (e.g., abrupt jumps from 66.9° to 144.7°, followed by minimal changes from 144.7° to 150.9° in Figure 6e). Consequently, conclusions about the optimal wettability for TPI performance often lean inaccurately toward excessively high hydrophobicity. This tendency arises because increases in doping at certain stages disproportionately amplify hydrophobicity.

To overcome this limitation, wettability itself should be treated as the variable of interest and independent of uniform doping levels, to uncover more meaningful insights. For instance, Zhang et al. directly varied the wettability of Au/C GDEs by regulating the contact angles and evaluated their eCO_2RR performance (Figure 6f,g).[43] In situ fluorescence electrochemical spectroscopy further quantified CO_2 transport behavior at the interface, revealing the pivotal role of interfacial CO_2 transport in maintaining stable CO_2 equilibrium concentrations during electrochemical reactions (Figure 6h). This study, using wettability as a direct variable, provides more valuable guidance for leveraging hydrophobicity to optimize TPI and facilitates catalytic processes effectively. In addition, composite hydrophobic strategies can facilitate a deeper exploration of wettability regulation. For instance, in coating-based methods, blending multiple hydrophobic polymers with intrinsically different wettabilities and carefully adjusting their proportions enable more precise and versatile control of surface wettability. In doping-based methods, integrating materials, such as PTFE (to enhance hydrophobicity) and carbon black (to improve conductivity), helps to achieve a more optimized balance between hydrophobic performance and electrical conductivity; 3) Regulating the wettability of TPIs significantly influences product selectivity in eCO_2RR, as different products require distinct TPI environments, determined by the specific CO_2-to-proton concentration ratio needed for optimal selectivity. For instance, it has been demonstrated that high CO_2/proton ratios favor the generation of C_{2+} products.[44] By carefully tuning the TPI wettability, the CO_2/proton concentration ratio at the interface can be precisely controlled, thereby affecting the product distribution.[42] Similarly, Han et al. showed that adjusting the CO_2/proton ratio could significantly improve ethanol selectivity (Figure 1a).[19] Thus, while regulating wettability, it is crucial to align adjustments with the target product, ensuring the required CO_2/proton ratio is achieved for optimal selectivity. d) In addition, the wettability of TPI may alter during the electrochemical testing. As shown in Table 1, although many strategies successfully tune the GDE interface to be superhydrophobic, a decrease in hydrophobicity is commonly observed after reaction. This highlights the importance of considering the effects of electrowetting on interfacial stability when studying TPI modulation through wettability. Employing dielectric hydrophobic materials is one effective strategy to mitigate these effects and maintain interface stability.[7a,45] Real-time monitoring is equally crucial. Under actual operating conditions, techniques such as electrochemical impedance spectroscopy and optical microscopy, can be employed to dynamically observe wettability states. Building on this, the development of potential-dependent strategies for dynamically tuning wettability could further help maintain an optimal TPI during continuous operation.

Here, we highlight the pivotal role of proper wettability control in optimizing TPI construction toward further electrocatalytic performance optimization, not only for eCO_2RR but also for various electrochemical reactions that involve gaseous reactants.[11,12]

6. Summary

In summary, this concept traces the evolution of catalytic interface configurations from the traditional liquid–solid DPI to the advanced gas–liquid–solid TPI in eCO_2RR. We outline the major challenges associated with constructing TPIs on eCO_2RR GDEs and review recent advancements in enhancing TPI stability and enrichment, which include hydrophobic polymer/molecular modifications and hierarchical structure fabrication to improve hydrophobicity. However, most current studies focus excessively on achieving superhydrophobicity, which, while effective in improving activity, selectivity, and stability, introduces new challenges, such as electrolyte repulsion and insufficient proton accessibility. We identify the factors contributing to excessively high hydrophobicity in these strategies and propose solutions to address these limitations.

The pivotal role of wettability-controlled TPIs in eCO_2RR remains inadequately explored. To better regulate TPI through wettability engineering, we propose the following principles: 1) Prioritize maximizing the TPI rather than focusing solely on hydrophobicity enhancement, HER suppression, or local CO_2 concentration increase; a combination of strategies may yield superior results. 2) Treat wettability changes as direct variables rather than linking them indirectly to the content of hydrophobic modification materials. 3) Leverage proper wettability modulation to not only enhance TPI formation but also to control product selectivity by optimizing the CO_2/proton ratio. 4) Consider the dynamic changes in TPI wettability during electrocatalysis and ensures its stability alongside consistent catalytic performance.

We hope this work provides valuable insights and inspiration for the rational design of three-phase systems for wettability-regulated eCO_2RR and other gas-involved electrochemical processes, paving the way for further advancements in sustainable energy technologies.

Acknowledgements

J.Y. acknowledges financial support from Hong Kong Polytechnic University (P0042930, P0050410 and P0053682), Research Grants Council of the Hong Kong Special Administrative (SAR) Region, China (Project No. PolyU 25300823 and PolyU 15300724), and National Natural Science Foundation of China (62422512). Q.L. acknowledges financial support from the Science and Technology Development Fund of the Macau SAR, China (No. 0056/2024/RIB1).

Conflict of Interest

The authors declare no conflict of interest.

Keywords: electroreduction of CO_2 · interface engineering · wettabilities

[1] a) S. Gao, Y. Lin, X. Jiao, Y. Sun, Q. Luo, W. Zhang, D. Li, J. Yang, Y. Xie, *Nature* **2016**, *529*, 68; b) B. A. Rosen, A. Salehi-Khojin, M. R. Thorson, W. Zhu, D. T. Whipple, P. J. A. Kenis, R. I. Masel, *Science* **2011**, *334*, 643; c) Q. Lei, L. Huang, J. Yin, B. Davaasuren, Y. Yuan, X. Dong, Z.-P. Wu, X. Wang, K. X. Yao, X. Lu, *Nat. Commun.* **2022**, *13*, 4857.

[2] a) D. Wakerley, S. Lamaison, J. Wicks, A. Clemens, J. Feaster, D. Corral, S. A. Jaffer, A. Sarkar, M. Fontecave, E. B. Duoss, *Nat. Energy* **2022**, *7*, 130; b) Q. Lei, H. Zhu, K. Song, N. Wei, L. Liu, D. Zhang, J. Yin, X. Dong, K. Yao, N. Wang, *J. Am. Chem. Soc.* **2020**, *142*, 4213.

[3] J. Jin, J. Wicks, Q. Min, J. Li, Y. Hu, J. Ma, Y. Wang, Z. Jiang, Y. Xu, R. Lu, *Nature* **2023**, *617*, 724.

[4] Y. Zhao, L. Hao, A. Ozden, S. Liu, R. K. Miao, P. Ou, T. Alkayyali, S. Zhang, J. Ning, Y. Liang, *Nat. Synth.* **2023**, *2*, 403.

[5] a) S. Jin, Z. Hao, K. Zhang, Z. Yan, J. Chen, *Angew. Chem. Int. Ed.* **2021**, *133*, 20795; b) L. Huang, Z. Liu, G. Gao, C. Chen, Y. Xue, J. Zhao, Q. Lei, M. Jin, C. Zhu, Y. Han, *J. Am. Chem. Soc.* **2023**, *145*, 26444.

[6] U. O. Nwabara, A. D. Hernandez, D. A. Henckel, X. Chen, E. R. Cofell, M. P. De-Heer, S. Verma, A. A. Gewirth, P. J. A. Kenis, *ACS Appl. Energy Mater.* **2021**, *4*, 5175.

[7] a) A. Wagner, C. D. Sahm, E. Reisner, *Nat. Catal.* **2020**, *3*, 775; b) X. Chen, C. Chen, Y. Wang, Z. Pan, J. Chen, Y. Xu, L. Zhu, T. Song, R. Li, L. Chen, *Chem. Eng. J.* **2024**, *482*, 148944.

[8] W. Zhang, A. Yu, H. Mao, G. Feng, C. Li, G. Wang, J. Chang, D. Halat, Z. Li, W. Yu, *J. Am. Chem. Soc.* **2024**, *146*, 21335.

[9] T. Burdyny, W. A. Smith, *Energy Environ. Sci.* **2019**, *12*, 1442.

[10] W. Lai, Y. Qiao, Y. Wang, H. Huang, *Adv. Mater.* **2023**, *35*, 2306288.

[11] J. Ryu, D. W. Lee, *J. Mater. Chem. A* **2024**, *12*, 10012.

[12] M. Li, M. N. Idros, Y. Wu, T. Burdyny, S. Garg, X. S. Zhao, G. Wang, T. E. Rufford, *J. Mater. Chem. A* **2021**, *9*, 19369.

[13] a) K. Liu, W. A. Smith, T. Burdyny, *ACS Energy Lett.* **2019**, *4*, 639; b) D. Higgins, C. Hahn, C. Xiang, T. F. Jaramillo, A. Z. Weber, *ACS Energy Lett.* **2018**, *4*, 317.

[14] a) S. Li, X. Dong, G. Wu, Y. Song, J. Mao, A. Chen, C. Zhu, G. Li, Y. Wei, X. Liu, *Nat. Commun.* **2024**, *15*, 6101; b) F. P. García de Arquer, C.-T. Dinh, A. Ozden, J. Wicks, C. McCallum, A. R. Kirmani, D.-H. Nam, C. Gabardo, A. Seifitokaldani, X. Wang, *Science* **2020**, *367*, 661.

[15] Z. Xing, L. Hu, D. S. Ripatti, X. Hu, X. Feng, *Nat. Commun.* **2021**, *12*, 136.

[16] L. Zhang, Z. Wei, S. Thanneeru, M. Meng, M. Kruzyk, G. Ung, B. Liu, J. He, *Angew. Chem. Int. Ed.* **2019**, *131*, 15981.

[17] B. Han, X. Tong, P. Zhang, P. Chen, Z. He, X. Kang, Y. Yin, Y. Cheng, M. Zhou, L. Jing, *Angew. Chem. Int. Ed.* **2024**, *64*, e202413005.

[18] S.-H. Li, S. Hu, H. Liu, J. Liu, X. Kang, S. Ge, Z. Zhang, Q. Yu, B. Liu, *ACS Nano* **2023**, *17*, 9338.

[19] Z. Xing, X. Hu, X. Feng, *ACS Energy Lett.* **2021**, *6*, 1694.

[20] a) Y. Lin, T. Wang, L. Zhang, G. Zhang, L. Li, Q. Chang, Z. Pang, H. Gao, K. Huang, P. Zhang, *Nat. Commun.* **2023**, *14*, 3575; b) D. Wakerley, S. Lamaison, F. Ozanam, N. Menguy, D. Mercier, P. Marcus, M. Fontecave, V. Mougel, *Nat. Mater.* **2019**, *18*, 1222; c) N. Qiu, W. Lu, H.-Q. Wang, *Rare Met.* **2024**, *44*, 1.

[21] S. Yu, X. Li, J. Li, S. Liu, W. Lu, Z. Shao, B. Yi, *Energy Convers. Manage.* **2013**, *76*, 301.

[22] M. W. Cross, W. J. Varhue, M. R. McDevitt, D. L. Hitt, *Adv. Chem. Engineer. Sci.* **2016**, *6*, 541.

[23] J. Park, H. Oh, T. Ha, Y. I. Lee, K. Min, *Appl. Energy* **2015**, *155*, 866.

[24] Z.-Z. Niu, F.-Y. Gao, X.-L. Zhang, P.-P. Yang, R. Liu, L.-P. Chi, Z.-Z. Wu, S. Qin, X. Yu, M.-R. Gao, *J. Am. Chem. Soc.* **2021**, *143*, 8011.

[25] M. N. Idros, M. Li, Y. Wu, T. E. Rufford, *Chemeca 2021: Advance, Disrupt and Sustain: Advance, Disrupt and Sustain*, Engineers Australia Barton, ACT **2021**.

[26] C.-T. Dinh, T. Burdyny, M. G. Kibria, A. Seifitokaldani, C. M. Gabardo, F. P. García de Arquer, A. Kiani, J. P. Edwards, P. De Luna, O. S. Bushuyev, *Science* **2018**, *360*, 783.

[27] G. Park, S. Hong, M. Choi, S. Lee, J. Lee, *Catal. Today* **2020**, *355*, 340.

[28] M. Wang, Z. Wang, Z. Huang, M. Fang, Y. Zhu, L. Jiang, *ACS Nano* **2024**, *18*, 15303.

[29] M. Wang, L. Wan, J. Luo, *Nanoscale* **2021**, *13*, 3588.

[30] D. M. Koshy, S. A. Akhade, A. Shugar, K. Abiose, J. Shi, S. Liang, J. S. Oakdale, S. E. Weitzner, J. B. Varley, E. B. Duoss, *J. Am. Chem. Soc.* **2021**, *143*, 14712.

[31] P. An, L. Wei, H. Li, B. Yang, K. Liu, J. Fu, H. Li, H. Liu, J. Hu, Y.-R. Lu, *J. Mater. Chem. A* **2020**, *8*, 15936.

[32] X. Zhao, H. Xie, B. Deng, L. Wang, Y. Li, F. Dong, *Chem. Commun.* **2024**, *60*, 542.

[33] M. Sun, J. Cheng, M. Yamauchi, *Nat. Commun.* **2024**, *15*, 491.

[34] Z. Wei, S. Yan, J. Lin, Q. Hu, Y. Cui, Q. Wang, Z. Li, Z. Cheng, *ACS Sustain. Chem. Eng.* **2024**, *12*, 16453.

[35] H.-Q. Liang, S. Zhao, X.-M. Hu, M. Ceccato, T. Skrydstrup, K. Daasbjerg, *ACS Catal.* **2021**, *11*, 958.

[36] R. Shi, X. Zhang, C. Li, Y. Zhao, R. Li, G. I. N. Waterhouse, T. Zhang, *Sci. Adv.* **2024**, *10*, eadn0947.

[37] S. Shu, T. Song, C. Wang, H. Dai, L. Duan, *Angew. Chem. Int. Ed.* **2024**, e202405650.

[38] X. Sheng, W. Ge, H. Jiang, C. Li, *Adv. Mater.* **2022**, *34*, 2201295.

[39] Y.-J. Ko, C. Lim, J. Jin, M. G. Kim, J. Y. Lee, T.-Y. Seong, K.-Y. Lee, B. K. Min, J.-Y. Choi, T. Noh, *Nat. Commun.* **2024**, *15*, 3356.

[40] X. Zhang, F. Shi, X. Yu, H. Liu, Y. Fu, Z. Wang, L. Jiang, X. Li, *J. Am. Chem. Soc.* **2004**, *126*, 3064.

[41] J. W. Bai, W. S. Wang, J. Liu, *Chem. Eur. J.* **2023**, *29*, e202302461.

[42] M. Fang, M. Wang, Z. Wang, Z. Zhang, H. Zhou, L. Dai, Y. Zhu, L. Jiang, *J. Am. Chem. Soc.* **2023**, *145*, 11323.

[43] H. Rabiee, L. Ge, J. Zhao, X. Zhang, M. Li, S. Hu, S. Smart, T. E. Rufford, Z. Zhu, H. Wang, *Appl. Catal. B: Environ.* **2022**, *310*, 121362.

[44] C. Kim, J. C. Bui, X. Luo, J. K. Cooper, A. Kusoglu, A. Z. Weber, A. T. Bell, *Nat. Energy.* **2021**, *6*, 1026.

[45] K. Wagner, P. Tiwari, G. F. Swiegers, G. G. Wallace, *Energy Environ. Sci.* **2018**, *11*, 172.

[46] R. Shi, J. Guo, X. Zhang, G. I. N. Waterhouse, Z. Han, Y. Zhao, L. Shang, C. Zhou, L. Jiang, T. Zhang, *Nat. Commun.* **2020**, *11*, 3028.

[47] K. Junge Puring, D. Siegmund, J. Timm, F. Möllenbruck, S. Schemme, R. Marschall, U. P. Apfel, *Adv. Sustain. Syst.* **2021**, *5*, 2000088.

[48] L. Xiong, X. Fu, Y. Zhou, P. Nian, Z. Wang, Q. Yue, *ACS Catal.* **2023**, *13*, 6652.

[49] L. Zhou, C. Li, J. J. Lv, W. Wang, S. Zhu, J. Li, Y. Yuan, Z. J. Wang, Q. Zhang, H. Jin, *Carbon Energy* **2023**, *5*, e328.

[50] Z.-Z. Niu, F.-Y. Gao, X.-L. Zhang, P.-P. Yang, R. Liu, L.-P. Chi, Z.-Z. Wu, S. Qin, X. Yu, M.-R. Gao **2021**, *143*, 8011.

[51] Y. Wu, J. Feng, D. Shi, W. Zhang, Y. Tang, Q. Gao, *Chem. Commun.* **2023**, *59*, 10428.

Manuscript received: December 9, 2024
Revised manuscript received: April 13, 2025
Version of record online: May 2, 2025